

# Effect of Particle Size in Aviation Turbine Fuel- $\text{Al}_2\text{O}_3$ Nanofluids for Heat Transfer Applications

Sandipkumar Sonawane, Upendra Bhandarkar, Bhalchandra Puranik, S. Sunil Kumar

**Abstract**—The effect of Alumina nanoparticle size on thermophysical properties, heat transfer performance and pressure loss characteristics of Aviation Turbine Fuel (ATF)- $\text{Al}_2\text{O}_3$  nanofluids is studied experimentally for the proposed application of regenerative cooling of semi-cryogenic rocket engine thrust chambers.  $\text{Al}_2\text{O}_3$  particles with mean diameters of 50 nm or 150 nm are dispersed in ATF. At 50°C and 0.3% particle volume concentration, the bigger particles show increases of 17% in thermal conductivity and 55% in viscosity, whereas the smaller particles show corresponding increases of 21% and 22% for thermal conductivity and viscosity respectively. Contrary to these results, experiments to study the heat transfer performance and pressure loss characteristics show that at the same pumping power, the maximum enhancement in heat transfer coefficient at 50°C and 0.3% concentration is approximately 47% using bigger particles, whereas it is only 36% using smaller particles.

**Keywords**—Heat transfer performance, Nanofluids, Thermal conductivity, Viscosity

## I. INTRODUCTION

CONVENTIONAL heat transfer fluids with dispersed ultra fine particles of nanometer size are called nanofluids [1]. Numerous experimental studies on water- $\text{Al}_2\text{O}_3$  nanofluids have shown significant enhancement in thermal conductivity and heat transfer performance when nanofluids are used. Chandrasekar et al. [2] measured 9.7% enhancement in thermal conductivity for water- $\text{Al}_2\text{O}_3$  nanofluids with a particle volume concentration of 3%. Yoo et al. [3] obtained an enhancement of 4% in the thermal conductivity of water- $\text{Al}_2\text{O}_3$  nanofluids at 1% particle volume concentration. Wang et al. [4] measured an enhancement of 16% in the thermal conductivity of water- $\text{Al}_2\text{O}_3$  nanofluids at 5.5% particle volume concentration. Das et al. [5] found that the thermal conductivity of nanofluids increases with increasing temperature as well as with increasing particle concentration. They obtained an enhancement of 9.4% in the thermal conductivity at 21°C and an enhancement of 24.3% at 51°C for water- $\text{Al}_2\text{O}_3$  nanofluids at 4% volume concentration of nanoparticles.

In order to use nanofluids as working fluids for practical applications in the turbulent regime, the heat transfer performance and pressure loss characteristics have also been investigated by several researchers [6]-[9]. Heat transfer and

fluid flow characteristics of water- $\text{Al}_2\text{O}_3$  and water- $\text{TiO}_2$  nanofluids were experimentally investigated by Pak and Cho [6]. Their experimental results showed that the Nusselt number of a nanofluid increases with an increase in the Reynolds number as well as with an increase in the particle concentration up to 3%. They proposed a heat transfer correlation for the determination of the heat transfer coefficient for the nanofluids based on their experimental results. Xuan and Li [7] experimentally studied the convective heat transfer performance and fluid flow characteristics for water-Cu nanofluids flowing in a straight tube under laminar and turbulent flow conditions. They obtained an enhancement of 39% in the heat transfer coefficients using nanofluids at 2% concentration by volume. Xuan and Li proposed a correlation for the determination of the heat transfer coefficient based on their results. Duangthongsuk and Wongwises [8] obtained 26% enhancement in the heat transfer coefficient at 1% particle volume concentration using water- $\text{TiO}_2$  nanofluids flowing in a horizontal double tube heat exchanger under turbulent flow conditions. Farajollahi et al. [9] investigated heat transfer characteristics of water- $\text{Al}_2\text{O}_3$  and water- $\text{TiO}_2$  nanofluids flowing in a shell and tube heat exchanger under turbulent flow conditions. The experimental results for both nanofluids showed that the heat transfer characteristics of nanofluids significantly improve with Peclet number.

The objective of the present study is to investigate the effect of particle size on heat transfer performance of ATF- $\text{Al}_2\text{O}_3$  nanofluids for its potential application of regenerative cooling of the thrust chambers of semi-cryogenic rocket engines. Semi-cryogenic rocket engines use ATF as the fuel and liquid oxygen as the oxidizer. The fuel is usually used to regeneratively cool the combustion chamber wall before it is introduced inside the chamber. For better regenerative heat transfer performance of the ATF it is proposed to add  $\text{Al}_2\text{O}_3$  nanoparticles to it.

## II. NANOFLUID PREPARATION

A stable ATF- $\text{Al}_2\text{O}_3$  nanofluid is prepared using a two-step method [10].  $\text{Al}_2\text{O}_3$  nanoparticles with average particle size 50 nm and 150 nm are obtained commercially (Nanostructured & Amorphous Materials Inc., USA). Oleic acid and 'Tween' 20 LR are used as surfactants to reduce the tendency of agglomeration of nanoparticles in the base fluid. Several trials are carried out to decide the appropriate concentration of surfactants to be used to obtain a stable nanofluid solution. It is found that the nanofluid with  $\text{Al}_2\text{O}_3$  particles of size 150 nm

Sandipkumar Sonawane, Upendra Bhandarkar and Bhalchandra Puranik are with the Mechanical Engineering Department, Indian Institute of Technology, Bombay, Mumbai 400076 India (phone: +91-22-25764533; fax: +91-22-25726875; e-mail: sandipsonawane@iitb.ac.in).

S. Sunil Kumar is with Liquid Propulsion Systems Center, Indian Space Research Organization (ISRO), Valiamala 695547 India (e-mail: sunil\_plamood@yahoo.com).

and at 0.1% concentration remains stable for 6 hours after 12 hrs of sonication, if prepared using 0.18 ml each of Oleic acid and 'Tween' 20 LR for 1000 ml ATF. A higher concentration of surfactants (0.26 ml each of Oleic acid and 'Tween' 20 LR for 1000 ml ATF) is required for preparation of nanofluids with the smaller nanoparticles at 0.1% particle volume concentration. The higher surface area of smaller particles thus necessitates a higher amounts of surfactants for a given particle volume concentration.

### III. EXPERIMENTAL APPARATUS

#### Thermal Conductivity Measurement

The thermal conductivity of nanofluids is measured using the transient hot wire method, which is one of the most accurate and widely used methods for measurement of thermal conductivity of fluids [11]. The schematic diagram of transient hot wire apparatus designed and fabricated in-house for this purpose is shown in Fig. 1.

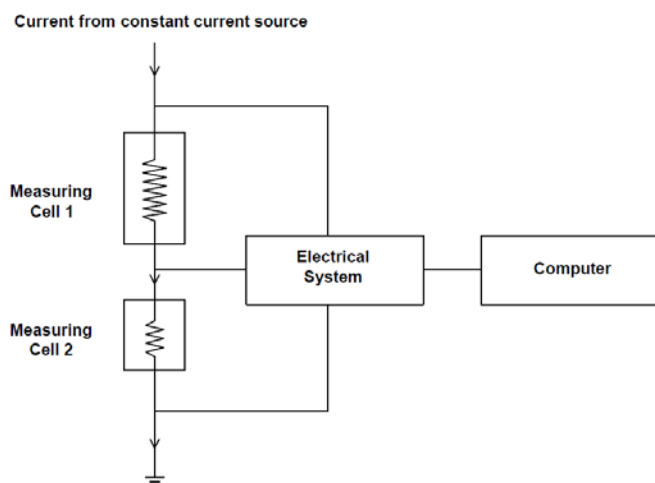


Fig. 1 Schematic diagram of the transient hot wire apparatus to measure the thermal conductivity of nanofluids

The apparatus consists of two measuring cells (to compensate for finite length losses [12]) of lengths 15 cm and 10 cm, an electrical system and a computer. The diameter of each measuring cell is 50 mm. Platinum wires with diameter of 50.8  $\mu\text{m}$  are soldered between brass nuts and bolts in their respective cells. The temperature coefficient of resistivity for the platinum wire is  $0.003729/^{\circ}\text{C}$ . The ratio of length to diameter of platinum wire is kept sufficiently large to eliminate axial conduction at both ends of the wire. Both ends of the measuring cells are connected to an electrical system which measures the voltage drop across the wires at specific time intervals. The temperature of the nanofluid stored in the measuring cells is measured using calibrated 'K' type thermocouples. The thermal conductivity of the ATF- $\text{Al}_2\text{O}_3$  nanofluids at particle volume concentration of 0.1 and 0.3% ( $30^{\circ}\text{C}$ - $50^{\circ}\text{C}$ ) is calculated using the following equation [12], [13].

$$K = \frac{q}{4\pi\Delta T} \ln\left(\frac{t_2}{t_1}\right), \quad (1)$$

where K is the thermal conductivity, q is the applied electric power per unit length of the wire, and  $\Delta T$  is the temperature rise of the wire between time  $t_1$  and  $t_2$ .

#### Convective Heat Transfer Coefficient and Pressure Drop Measurement

The schematic diagram of the experimental set-up fabricated for measuring the convective heat transfer coefficient and pressure drop is shown in Fig. 2. The experimental set-up mainly includes a gear pump, a mass flow meter, test section, viscometer, differential pressure gauge (DPG) and chilling unit. The test section (1.77 m long) is a double tube counter flow exchanger where nanofluid passes through the inner copper tube (6 mm inner diameter, 1 mm thickness) and hot water flows through the annular section. The outer tube is made of stainless steel with 18 mm inner diameter and 4.5 mm thickness. The hydrodynamic entry length is kept sufficiently large (i.e.,  $x/d=150$ ) in order to ensure fully developed turbulent flow at the entrance of the test section. Four thermocouples are used to measure inlet and outlet temperatures of hot water and nanofluid. A Differential Pressure Gauge (DPG) (0-2  $\text{kg}/\text{cm}^2$ , Waaree Instruments) is mounted along the test section for the measurement of pressure drop. The temperatures recorded by thermocouples are directly sent to the computer via a data logger. The mass flow rate of the nanofluid is controlled by operating the bypass valve. The mass flow rate and density are measured using a Coriolis mass flow and density meter (Rota Yokogawa GmbH & Co., Germany). The heated nanofluid in the test section is cooled using the chilling unit. The flow rate of hot water is measured using a catch and time method.

#### Viscosity Measurement

Micro Motion 7829 visconic viscosity meter (Emerson process management) is used for the measurement of dynamic viscosity of nanofluids. It is mounted in the experimental set-up shown in Fig. 2. It is a digital viscosity meter that uses a tuning fork. The viscosity and density of the fluid are determined from the resonance of the tuning fork immersed in the fluid. A temperature sensor (RTD) is also fitted to measure the temperature of the fluid. The tuning fork of the viscometer is inserted in the mixing chamber as shown in Fig. 2. The readings of dynamic viscosity recorded by the viscometer with a time interval of 1 second are sent to the computer via RS 232-RS 485 converter. The viscometer can also measure the temperature and density of the fluid inside the mixing chamber.

#### Specific Heat Measurement

The schematic diagram of a calorimeter fabricated for measurement of the specific heat of the nanofluid is shown in Fig. 3. It consists of an inside copper vessel which is filled with known quantity of hot water. The outer plastic vessel is

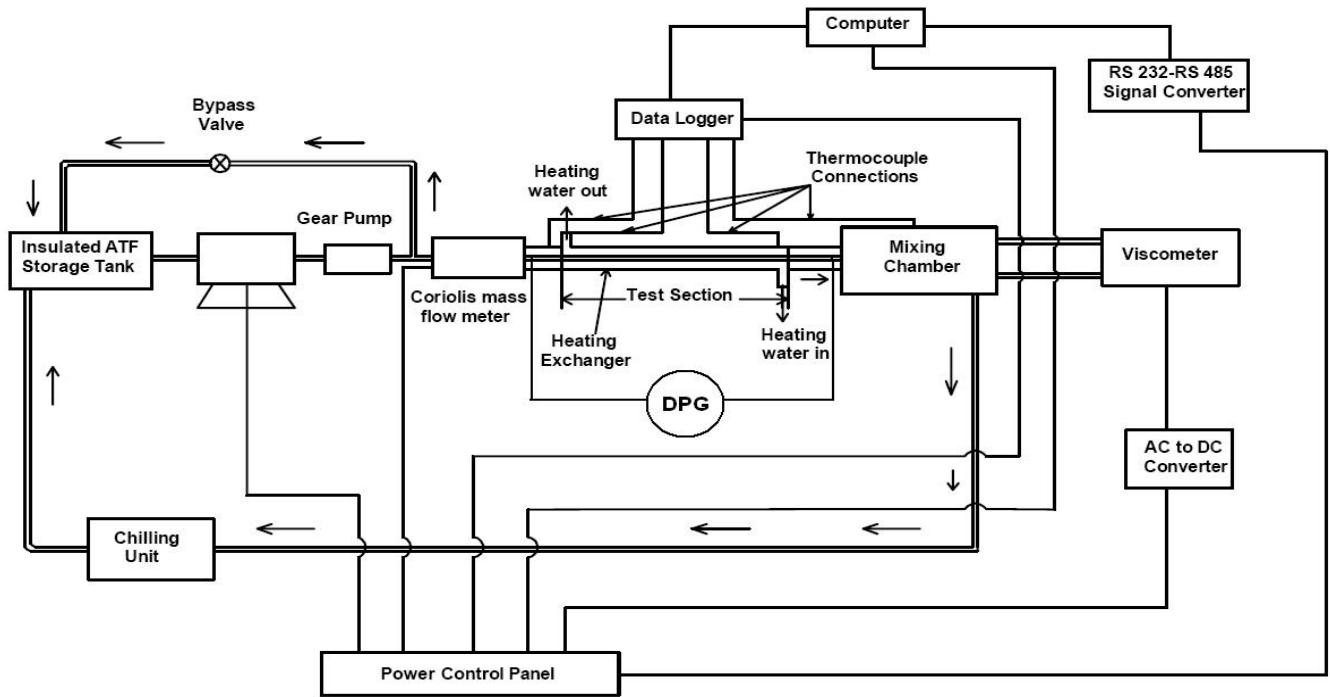


Fig. 2 Schematic diagram of the experimental set-up for convective heat transfer coefficient and pressure drop measurement

filled with nanofluid whose specific heat is to be determined. The outer plastic vessel is properly insulated in order to reduce the effect of ambient conditions on the heat transfer mechanism. Hot water and nanofluid are stirred continuously using the stirring mechanisms shown in Fig. 3. Eight thermocouples are used to measure temperatures of the inner fluid and nanofluid. The thermocouples are connected to a data logger and temperatures at a time interval of 1 second are recorded.

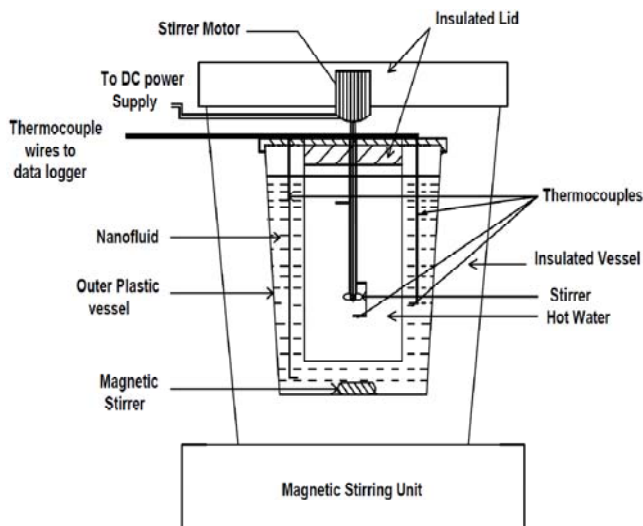


Fig. 3 Schematic diagram of the calorimeter for specific heat measurement

#### IV. DATA REDUCTION

The heat transfer coefficient of nanofluid with 0.1% and 0.3% particle volume concentrations and at various Reynolds number are determined. The thermophysical properties of the nanofluid are determined at mean bulk temperature (50°C). The procedure used for measurement of heat transfer coefficient is explained as follows.

The heat transfer rate for heating the nanofluid is given as

$$\dot{Q} = \dot{m}_{nf} C_{p,nf} (T_{(out)nf} - T_{(in)nf}), \quad (2)$$

where  $\dot{m}_{nf}$ ,  $T_{(out)nf}$  and  $T_{(in)nf}$  are measured directly as mentioned in section III(B). The specific heat  $C_{p,nf}$  of the nanofluid is evaluated using data from the calorimeter. The overall heat transfer coefficient based on the inner tube area ( $U_i$ ) is calculated from

$$\dot{Q} = U_i A_i (LMTD), \quad (3)$$

where  $\dot{Q}$  is the same as in Eq. 2. By substituting values of thermophysical properties of hot water at the mean bulk temperature [14], the Reynolds and Prandtl numbers for water are determined using the expressions

$$Re_w = \frac{\rho_w u_w (D_i - d_o)}{\mu_w} \quad (4)$$

and

$$Pr_w = \frac{\mu_w C_{p,w}}{K_w}. \quad (5)$$

The Nusselt number for water is then determined using the Dittus-Boelter correlation [14]

$$Nu_w = 0.023Re_w^{0.8}Pr_w^{0.3}. \quad (6)$$

Using the values of Nusselt number of water, diameter of annular section ( $D_i - d_o$ ) and thermal conductivity of water ( $K_w$ ) at the mean bulk temperature [14], the outside heat transfer coefficient is determined using

$$Nu_w = \frac{h_o(D_i - d_o)}{K_w}. \quad (7)$$

The heat transfer coefficient for the nanofluid ( $h_i$ ) is determined using

$$\frac{1}{U_i} = \frac{1}{h_i} + \frac{d_i \ln \frac{d_o}{d_i}}{2K_{copper\ tube}} + \frac{d_i}{d_o} \times \frac{1}{h_o}, \quad (8)$$

where  $K_{copper\ tube}$  is thermal conductivity of tube material,  $d_i$  and  $d_o$  are the inside and outside diameters of tubes respectively.

The Nusselt number for the nanofluid ( $Nu_{nf}$ ) is calculated as

$$Nu_{nf} = \frac{h_i d_i}{K_{nf}}, \quad (9)$$

where  $h_i$  is the heat transfer coefficient of the nanofluid as determined from Eq. 9, and  $K_{nf}$  is the measured thermal conductivity of the nanofluid.

Using the measured pressure drop, the friction factor for the flow of nanofluids ( $f_{nf}$ ) is calculated using

$$f_{nf} = \frac{2d_i \Delta P_{nf}}{L \rho u^2}, \quad (10)$$

where  $\Delta P_{nf}$ ,  $d_i$ ,  $L$ ,  $\rho$  and  $u$  are pressure drop, inside diameter of inner tube, length of test section, density and mean velocity of nanofluids respectively.

## V. RESULTS AND DISCUSSION

### The Thermal Conductivity of Nanofluids

After validating the transient hot wire apparatus using toluene and deionized water [15], the thermal conductivities of plain ATF and the ATF- $Al_2O_3$  nanofluids are determined. The percentage enhancement in thermal conductivity as a function of temperature, for different particle volume concentrations (0.1% and 0.3%) and particle sizes (50 nm and 150 nm), is presented in Fig. 4. It can be observed from Fig. 4 that the enhancement in the thermal conductivity of ATF- $Al_2O_3$  nanofluids increases with particle volume concentration, decreases with increase in particle size and increases with increase in temperature. The experimental results show that the maximum enhancement in the thermal conductivity of ATF- $Al_2O_3$  nanofluids is 22% obtained using smaller particles (50 nm, 0.3% particle volume concentration and 50°C) which is higher than the enhancement obtained using bigger particles

for same conditions. These particle size dependent experimental results are consistent with theoretical thermal conductivity models [16], [17] and experimental studies [18], [19] of nanofluids. The significant enhancement in the thermal conductivity of nanofluids has been attributed to the Brownian motion of nanoparticles in the base fluid [5], [20]. At room temperature (i.e., 30°C), the experimental results show that the effect of particle size on the thermal conductivity enhancement is not remarkable. However as the temperature of nanofluids increases, the Brownian motion of nanoparticles in the base fluid increases which eventually results in a higher enhancement. The comparison between our experimental results and those predicted from a theoretical model [17] is presented in Fig. 5 as a function of particle size. It can be observed from Fig. 5 that the experimentally measured thermal conductivity enhancement values compare well with those obtained from the theoretical model [17] at a given particle concentration and temperature.

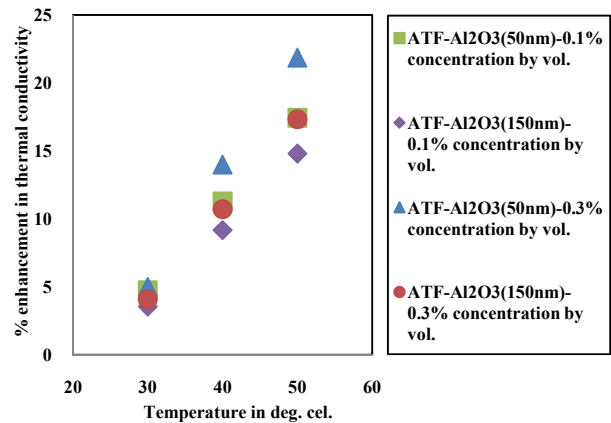


Fig. 4 Enhancement in the thermal conductivity of ATF- $Al_2O_3$  nanofluid as a function of temperature, for different particle volume concentrations (0.1% and 0.3%) and particle sizes (50 nm and 150 nm)

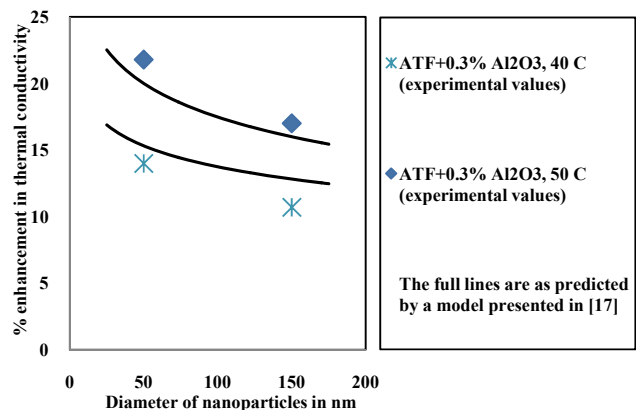


Fig. 5 Enhancement of thermal conductivity ATF- $Al_2O_3$  nanofluids as a function of particle size

### The Viscosity of Nanofluids

The dynamic viscosity of ATF- $Al_2O_3$  nanofluids as a function of temperature, for different particle volume

concentrations and particle sizes is presented in Fig. 6. It can be observed that the dynamic viscosity of nanofluids decreases with an increase in temperature, as expected [21]. It is found that the ATF- $\text{Al}_2\text{O}_3$  nanofluids using bigger particles show higher increase in viscosity when compared to the increase obtained using smaller particles. The experimental results for ATF- $\text{Al}_2\text{O}_3$  nanofluids are compared with similar experimental results for water- $\text{Al}_2\text{O}_3$  nanofluids [22], as a function of particle size, and this comparison has been presented in Fig. 7. It can be observed from Fig. 7 that the behavior of change in the viscosity of ATF- $\text{Al}_2\text{O}_3$  nanofluids with change in the particle size is qualitatively similar to the trend reported for other nanofluids.

The effect of particle volume concentration on percentage increase in viscosity is shown in Fig. 8. The experimental results show that the percentage increase in viscosity increases with increase in particle volume concentration at a given temperature due to increasing internal shear stresses [22].

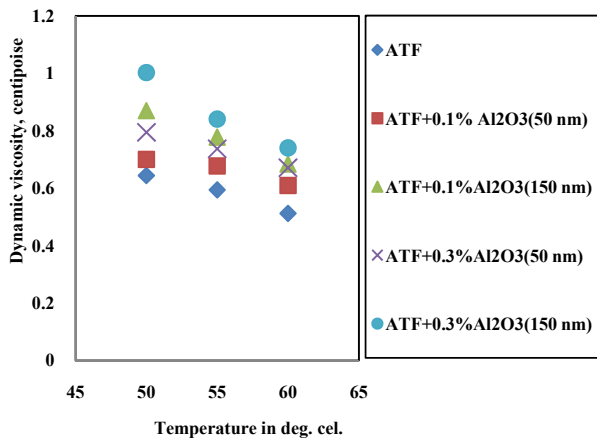


Fig. 6 Viscosity of ATF- $\text{Al}_2\text{O}_3$  nanofluid as a function of temperature, for different particle volume concentration and particle sizes

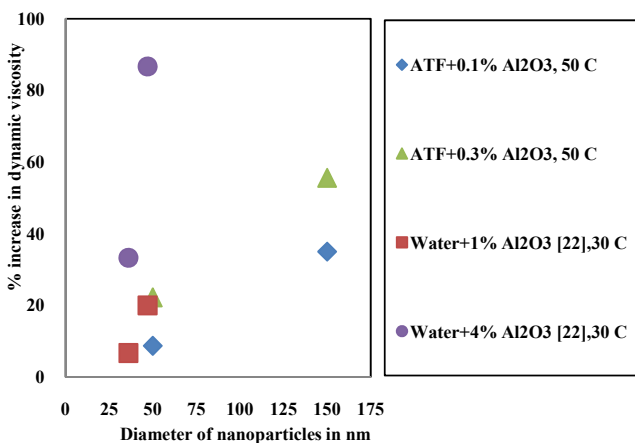


Fig. 7 Comparison of percentage increase in viscosity as a function of particle size with results from [22] for water- $\text{Al}_2\text{O}_3$  nanofluids

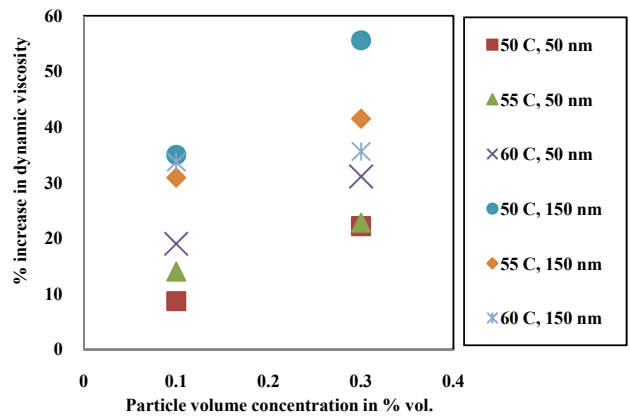


Fig. 8 Percentage enhancement in viscosity as a function of particle volume concentration, for different particle sizes and different temperatures

### The Specific Heat Measurement of Nanofluids

The specific heat of ATF- $\text{Al}_2\text{O}_3$  nanofluids is measured using the calorimeter shown in Fig. 3 at particle volume concentrations of 0.1% and 0.3% using both 50 nm and 150 nm particles. The specific heat of ATF- $\text{Al}_2\text{O}_3$  nanofluids as a function of particle volume concentration and for different particle sizes is shown in Fig. 9.

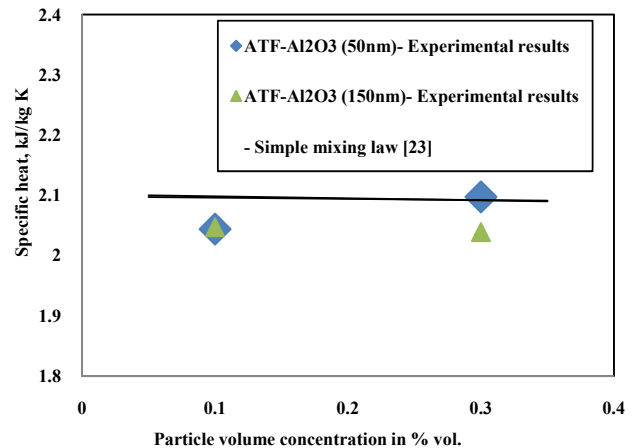


Fig. 9 Specific heat as a function of particle volume concentrations and particle size

The measured value of specific heat is compared with that obtained using a simple mixing law [23]. It can be observed that the experimental values of specific heat follow the values obtained from the mixing law. No significant effect of particle size and particle volume concentration on specific heat is observed.

### Heat Transfer Performance and Pressure Drop of Nanofluid

The validation of the experimental setup is carried out using water as working fluid. The measured values of the heat transfer coefficient are compared with those obtained using three well known empirical correlations, i.e., the Dittus-Boelter, Gneilinski and Sieder and Tate correlations [14], and good agreement is observed between the measured values and those obtained from the correlations.

After validation of the experimental setup, the effect of particle size on the convective heat transfer coefficient of the ATF- $\text{Al}_2\text{O}_3$  nanofluid is studied for particle volume concentrations of 0.1% and 0.3%. The mean temperature of the nanofluid during the experiments is  $50^\circ\text{C}$ . The experimental values of the convective heat transfer coefficient and those of the corresponding Nusselt number obtained using 50 nm or 150 nm particles are presented in Figs. 10 and 11 as a function of Reynolds number.

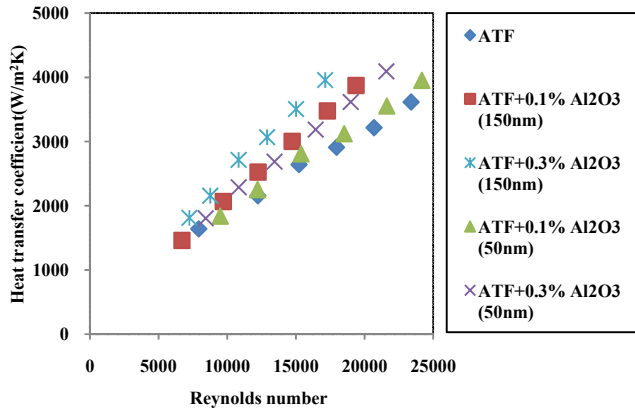


Fig. 10 Convective heat transfer coefficient of ATF- $\text{Al}_2\text{O}_3$  nanofluids as a function of Reynolds number for different particle volume concentrations and particle sizes

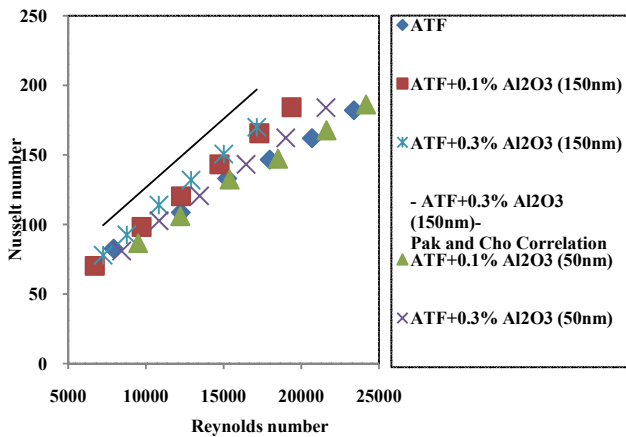


Fig. 11 Nusselt number of ATF- $\text{Al}_2\text{O}_3$  nanofluids as a function of Reynolds number at different particle volume concentrations and particle sizes

The experimental results show that both the heat transfer coefficient and the Nusselt number of the ATF- $\text{Al}_2\text{O}_3$  nanofluids increase with an increase in the Reynolds number as well as with an increase in the particle volume concentration. The convective heat transfer coefficient and the Nusselt number of the nanofluids are higher than those for the base fluid (ATF) at a given Reynolds number. It is found that the ATF- $\text{Al}_2\text{O}_3$  nanofluids using bigger particles show higher enhancement in the convective heat transfer coefficient than when using smaller particles at the same conditions. At 0.3% particle volume concentration and using bigger particles, approximately 33% enhancement in the heat transfer

coefficient and 15% enhancement in Nusselt number are observed at a given Reynolds number.

It can be observed from Fig. 11 that the experimental values of Nusselt number are lower than those predicted by the empirical Pak and Cho correlation [6] which was obtained using water- $\text{TiO}_2$  and water- $\text{Al}_2\text{O}_3$  nanofluids. The particle to base fluid interaction is possibly the reason for the observed deviation.

The effect of particle size on the heat transfer performance of the ATF- $\text{Al}_2\text{O}_3$  nanofluid is determined by calculating the ratio of experimental heat transfer coefficient for the nanofluid to that of ATF for the same pressure drop. This ratio is denoted as  $(h_{nf}/h_{ATF})_{\Delta P}$  and is evaluated for various Reynolds number of ATF. The calculated values of  $(h_{nf}/h_{ATF})_{\Delta P}$  obtained using 50 nm and 150 nm particles are presented in Fig. 12 as a function of Reynolds number of ATF. It can be observed that this ratio is higher than 1. It is found that the ATF- $\text{Al}_2\text{O}_3$  nanofluids with bigger particles show higher heat transfer performance than those with smaller particles. A similar calculation is performed for the Nusselt numbers and the results are presented in Fig. 13. The experimental results indicate that ATF- $\text{Al}_2\text{O}_3$  nanofluids with bigger particles (150 nm) always show better heat transfer performance when compared with pure ATF at the same pressure drop or pumping power. This result seems contradictory to the expectation especially after noting the percentage increases in thermal conductivity and viscosity [Figs. 4 and 8]. The smaller particles show a higher enhancement in thermal conductivity and a lower enhancement in viscosity. This would have implied that smaller particles would lead to lesser pressure drop and higher heat transfer enhancement for same volume fraction. Correspondingly, at the same pressure drop, the smaller particles should be expected to show an even higher enhancement in heat transfer performance. While this behavior requires a more detailed analysis and generation of extensive data, a preliminary explanation may be offered based on the nature of the flow. It is possible that for turbulent flows, the enhancement in thermal conductivity due to Brownian motion may not be significant, and the turbulent nature of the flow may dominate the heat transfer behavior. In this context, the bigger nanoparticles may promote disruption of the viscous sublayer of the turbulent boundary layer leading to a higher heat transfer performance.

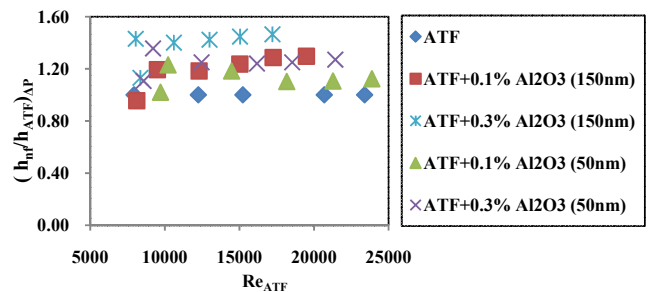


Fig. 12 Plot of ratio of convective heat transfer coefficient of ATF- $\text{Al}_2\text{O}_3$  nanofluids to that of ATF for same pressure drop, as a function of Reynolds number of ATF for different particle volume concentrations

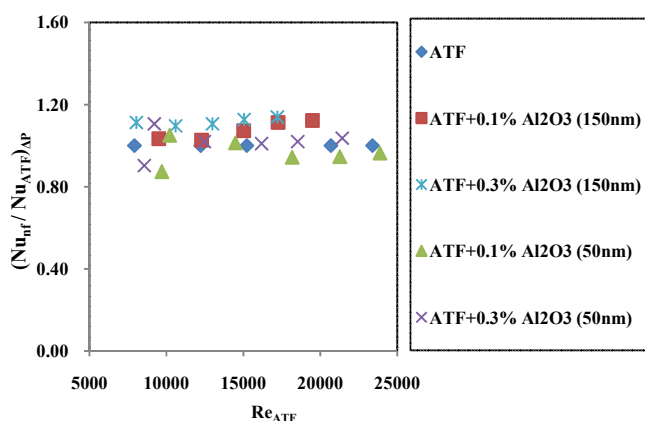


Fig. 13 Ratio of Nusselt number of ATF-Al<sub>2</sub>O<sub>3</sub> nanofluids to that of ATF as a function of Reynolds number of ATF for different particle volume concentrations

## VI. CONCLUSION

The effect of particle size on the thermophysical properties and heat transfer performance of ATF-Al<sub>2</sub>O<sub>3</sub> nanofluids has been evaluated experimentally in the present study. The effect of particle size on thermal conductivity enhancement is observed only at higher temperature (50<sup>0</sup>C). Though the nanofluids with bigger particles exhibit a higher increase in viscosity, they show better heat transfer performance when compared to smaller particles at the given conditions. For the same value of pressure drop, the use of ATF-Al<sub>2</sub>O<sub>3</sub> nanofluids with bigger particles enhances heat transfer performance up to 47% whereas the enhancement in heat transfer performance using smaller particles is up to 36% over pure ATF. Hence the selection of the particle size for the particular heat transfer application is a crucial aspect as it directly affects the economy of the thermal system.

## REFERENCES

- [1] S.U.S. Choi, J.A.Eastman, "Enhancing thermal conductivity of fluids with nanoparticles", ASME Int. Mech. Engg. Congress and Exh., Nov. 12-17, 1995, San Francisco, CA (US).
- [2] M.Chandrasekar, S.Suresh, A.Chandra Bose, "Experimental investigations and theoretical determination of thermal conductivity and viscosity of Al<sub>2</sub>O<sub>3</sub>/water nanofluid", Exp. Therm. Fluid Sci., vol. 34, pp. 210-216, Feb. 2010.
- [3] D.Yoo, K.S.Hong, H.Yang, "Study of thermal conductivity of nanofluids for the applications of heat transfer fluids", Thermochim. Acta, vol. 455, pp. 66-69, Apr. 2007.
- [4] X. Wang, X. Xu, S.U.S. Choi, "Thermal conductivity of nanoparticles-fluid mixture", J. Thermophys. Heat Transfer, vol. 13(4), pp. 474-480, Oct.-Dec. 1999.
- [5] S.K.Das, N.Putra, P.Theisen, W.Roetzel, "Temperature dependence of thermal conductivity enhancement of nanofluids", J. Heat Transfer, vol. 125, pp. 567-574, Aug. 2003.
- [6] B.C.Pak, Y.I.Cho, "Hydrodynamic and heat transfer study of dispersed fluids with submicron metallic oxide particles", Exp. Heat Transfer, vol. 11, pp.151-170, 1998.
- [7] Y.Xuan, Q.Li, "Investigation on convective heat transfer and flow features of nanofluids", ASME. J. Heat Transfer, vol. 125, pp. 151-155, Feb. 2003.
- [8] W. Duangthongsuk, S.Wongwises, "An experimental study on the heat transfer performance and pressure drop of TiO<sub>2</sub>-water nanofluids flowing under a turbulent flow regime", Int. J. Heat Mass Transfer, vol. 53, pp. 334-344, Jan. 2010.

- [9] B. Farajollahi, S.Gh.Etemad, M.Hojjat, "Heat transfer of nanofluids in a shell and tube heat exchanger", Int. J. Heat Mass Transfer, vol. 53, pp. 12-17, Jan. 2010.
- [10] W.Yu, D.M.France, J.L.Routbort, S.U.S.Choi, "Review and comparison of nanofluid thermal conductivity and heat transfer enhancements", Heat Transfer Engg., vol. 29(5), pp. 432-460, 2008.
- [11] S.M.S. Murshed, K.C.Leong, C.Yang, "Enhanced thermal conductivity of TiO<sub>2</sub>-water based nanofluids", Int. J. Therm. Sci., vol. 44, pp. 367-373, Apr. 2005.
- [12] C. Codreanu, N. Codreanu, V. Obreja, "An experimental approach of the hot wire method for measurement of the thermal conductivity", pp. 359-362, IEEE, 2006.
- [13] J.J.De Groot, J.Kestin, H.Sookiazian, "Instrument to measure thermal conductivity of gases", Physica, vol. 75, pp., 454-482, 1974.
- [14] F.P.Incropera, D.P.DeWitt, *Fundamentals of Heat and Mass Transfer*, 5<sup>th</sup> Edi. Wiley, Singapore, 2002.
- [15] M.L.V.Ramires, M.N.A.Fareleria, C.A.Nieto de Castro, M.Dix, W.A.Wakeham, "The thermal conductivity of toluene and water", Int. J. Thermophysics., vol. 14(6), pp. 1119-1130, 1993.
- [16] D.H.Kumar, H. Patel, V.R.Rajeev Kumar, T.Sundarrajan, T.Pradip, S.K.Das, "Model of heat conduction in nanofluids", Physical Rev. Lett., vol. 93 no. 14, 144301(1-4), Oct. 2004.
- [17] R.Prasher, P.Bhattacharya, P.Phelan, "Brownian-motion-based convective-conductive model for the effective thermal conductivity of nanofluids, Trans. ASME, vol. 128, pp. 588-595, June 2006.
- [18] S.Kim, S.Choi, D.Kim, "Thermal conductivity of metal-oxide nanofluids: particle size dependence and effect of laser irradiation", Trans. ASME, vol. 129, pp. 298-307, Mar. 2007.
- [19] C.Li,G.Peterson, "The effect of particle size on the effective thermal conductivity of Al<sub>2</sub>O<sub>3</sub>-water nanofluids", J. Appl. Phys., 101, 044312(1-5), 2007.
- [20] S.P. Jang, S.U.S. Choi, "Role of Brownian motion in the enhanced thermal conductivity of nanofluids", Appl. Phys. Lett., vol. 84, pp. 4316-4318, May 2004.
- [21] C.T.Nguyen,F.Desgranges,G.Roy,N.Galanis,T.Mare,S.Broucher, H. Angue Minsta, "Temperature and particle-size dependent viscosity data for water-based nanofluids-Hysteresis phenomenon", Int. J. Heat Fluid Flow, vol. 28, pp. 1492-1506, Dec. 2007.
- [22] C.T.Nguyen,F.Desgranges,N.Galanis,G.Roy,T.Mare,S.Broucher, H. Angue Minsta, "Viscosity data for Al<sub>2</sub>O<sub>3</sub>-water nanofluid-hysteresis: is heat transfer enhancement using nanofluids reliable?", Int. J. Ther. Sci., vol. 47, pp. 103-111, Feb. 2008.
- [23] P. Atkins and J. de Paula, *Physical chemistry*, 8<sup>th</sup> int. Edi. , New Delhi: Oxford University Press, 2006.